JOURNAL OF CATALYSIS 65, 390–401 (1980)

The Stoichiometry of Hydrogen and Carbon Monoxide Chemisorption on Alumina- and Silica-Supported Nickel

C. H. BARTHOLOMEW AND R. B. PANNELL

Department of Chemical Engineering, Brigham Young University, Provo, Utah 84602

Received November 19, 1979; revised April 14, 1980

Adsorption stoichiometries of H_2 at 298 K and CO at 190–298 K on alumina- and silica-supported Ni catalysts prepared by impregnation and precipitation techniques were investigated. In the case of alumina-supported nickel catalysts the metal loading was varied from 0.5 to 23 wt% in order to study the effects of metal–support interactions. Ni/SiO_2 catalysts were prepared by both impregnation and precipitation techniques to determine effects of catalyst preparation. Room-temperature H_2 adsorption on alumina- and silica-supported nickel occurs with a stoichiometry of one hydrogen atom per surface nickel atom as determined by chemisorption, X-ray diffraction, and electron microscopy. CO adsorption is considerably more complex, the stoichiometry of which varies with equilibration pressure, temperature, metal crystallite size, and metal loading. Formation of nickel carbonyl and substantial amounts of chemical and physical adsorption of CO on the support provide additional complications.

INTRODUCTION

Nickel catalysts find widespread industrial application in hydrogenation, hydrotreating, and steam reforming reactions. Recently considerable interest has developed in the application of nickel catalysts for methanation of coal synthesis gas (*1–5*). Despite this widespread use, there is unfortunately little consensus regarding measurement of nickel surface area.

In reviewing the pre-1975 literature dealing with measurement of metal surface areas, Farrauto (*6*) observed that nickel areas had been measured using hydrogen, oxygen, and carbon monoxide over a range of temperatures and pressures, and that the adsorption stoichiometries remained to be confirmed under well-defined conditions. In addition, he expressed the important need for developing a reproducible, standard technique for measuring nickel surface area.

In a recent paper (*7*), we reported the stoichiometries of hydrogen, carbon monoxide, and oxygen chemisorption on an unsupported nickel, the surface purity of which was established by ESCA measurements. Hydrogen adsorption was found to be well defined at room temperature over the pressure range of 100–400 Torr (1 Torr = 133.3 N m^{-2}), and the H/Ni_s ratio was found to be 1.0. Carbon monoxide adsorption, however, was determined to be considerably more complex, the stoichiometry depending greatly upon temperature and pressure. Nickel carbonyl formation was observed at 300 K. Oxygen adsorption was complicated by multilayer oxidation at 300 K and presumably molecular adsorption at 190 K.

Although adsorption of CO and H_2 on supported nickel has been the subject of numerous investigations (*6*), most of the previous work involved poorly characterized catalysts; for example, the extent of reduction of nickel to the metallic state was usually not measured and effects of metal loading and preparation technique were usually ignored. Moreover, nickel metal dispersions were either not determined or were determined using only one technique. In the course of this study we learned that all of these catalyst properties may influence adsorption stoichiometry. Thus, this present investigation was undertaken

0021-9517/80/100390-12$02.00/0

to determine the adsorption stoichiometries of hydrogen and carbon monoxide on well-characterized alumina- and silica-supported nickel and the effects of metal crystallite size, metal loading, degree of reduction to the metal, and preparation on adsorption of these gases.

EXPERIMENTAL

Equipment and Materials

Equipment. Gas adsorption measurements were carried out in a conventional Pyrex-glass volumetric adsorption apparatus capable of 10^{-6} Torr, obtained by means of oil diffusion and rotary pumps isolated from the adsorption system by a liquid-nitrogen-cooled trap. Each catalyst sample was placed in a Pyrex flow-through cell to enable reduction of samples in flowing hydrogen prior to the chemisorption measurement. The amount of gas adsorbed by the catalyst was determined by means of either a conventional gas burette connected to a mercury manometer backed by a metrically calibrated mirror or a Bourdon Gauge (Texas Instruments).

Materials. hydrogen gas (99.96%, Whitmore), purified by passing through an Engelhard palladium Deoxo catalytic purifier and a molecular sieve trap at 190 K, was used for both catalyst reduction and uptake measurements. Carbon monoxide (Matheson grade, 99.99%), high-purity helium (99.995%, Matheson), and nitrogen (99.99%, Whitmore) were used for carbon monoxide uptake measurements, dead volume, and passivation treatments, respectively.

Procedure

Catalyst preparation. Alumina-supported catalysts (with the exception of 2.9% Ni/Al_2O_3) were prepared by impregnation with a $Ni(NO_3)_2$ solution to incipient wetness of Kaiser SAS 5 × 8-mesh alumina (301 m^2/g) previously calcined 2 h at 873 K; after impregnation the catalysts were dried at 373 K in a forced-air-circulation oven for at least 24 h. Several impregnations were used in order to distribute the active catalytic material more uniformly through the internals of the support. Two Ni/SiO_2 catalysts were prepared by a similar impregnation of Cab-O-Sil (Cabot Corp.). Two other silica-supported catalysts and 2.9% Ni/Al_2O_3 were prepared by means of a controlled pH precipitation technique described by van Dillen *et al.* (*8*) using Cab-O-Sil and the same Kaiser alumina. These samples were also dried 24 h at 373 K.

Large samples (50–100 g) of each catalyst were reduced in a large reduction apparatus using flowing hydrogen at a space velocity of 1500–2000 h^{-1} according to a temperature schedule previously reported (*9*) followed by a 15-h hold at 725 K. After cooling to 298 K, the samples were passivated using a 1% air in N_2 stream at 2000–5000 h^{-1}. Percentage loadings were determined for most of the catalysts by Rocky Mountain Geochemical Corporation using atomic absorption spectroscopy.

Catalyst pretreatment. A standard pretreatment consisted of rereduction of a 1- to 3-g sample (previously reduced and passivated) in a small Pyrex cell at 723 K for 2–6 h followed by evacuation at 673 K for 1–2 h. This was in turn followed by measurement of H_2 and CO adsorption uptakes at 298 and 190 or 273 K, respectively.

Hydrogen and carbon monoxide chemisorption measurements. Because hydrogen adsorption on the support was found to be negligible at room temperature, total hydrogen uptake was measured at 298 K and no support correction was made. It was found that 45 min was sufficient to reach equilibrium (as determined from adsorption–time data).

Carbon monoxide adsorption was found to be considerably more complex than hydrogen adsorption. One major problem was the formation of nickel carbonyl at 298 K (*5, 10, 11*). However, it was found that by measuring the CO adsorption at 190 or 273 K, it was possible to essentially eliminate this problem. For safety purposes, after

each CO adsorption measurement the sample was evacuated and then heated from 190 or 273 to 575 K in flowing hydrogen to react any adsorbed CO to methane thereby avoiding nickel carbonyl formation.

Irreversible chemical adsorption of CO on the metallic constituents of each catalyst was measured according to the following method: (i) a known quantity of CO was admitted to the reduced and high-temperature evacuated sample at 190 or 273 K and allowed to equilibrate ½ h at 300–400 Torr (it was determined that CO uptake was strongly dependent on equilibration pressure and that equilibrium was approached more rapidly at these higher equilibration pressures), (ii) an adsorption isotherm was measured at this point representing the total adsorption on the catalyst—chemical and physical adsorption on the metal and on the support, (iii) the sample was evacuated for ½ h at 190 or 273 K to remove the physically adsorbed CO (it was determined that the effect of the evacuation time and pressure was negligible beyond ½ h and a pressure of 10^{-3} Torr, respectively), and (iv) CO was again admitted to the sample at 190 or 273 K, and after ½ h, another adsorption isotherm was measured. The last isotherm representing the total physical adsorption was subtracted from the first to obtain the chemically adsorbed CO. An additional correction for chemisorption on the support was determined by measuring the adsorption on pure alumina under conditions identical to those of the catalyst.

Calculations of surface area, dispersion, and average metal crystallite size for supported metals have been discussed by Bartholomew (*12, 13*). In this study, the site density of 6.77×10^{-2} nm^2/atom used in these calculations was based on an equal distribution of the three lowest index planes of nickel (fcc). In calculating metal dispersion (or the fraction of metal atoms exposed) the metal loading was multiplied by the fraction of nickel reduced to the metallic state, based on the assumption that unreduced nickel is present in a separate dispersed phase in intimate contact with the support. Thus the equation used to calculate dispersion was:

$$\% D = \frac{1.17X}{Wf}, \qquad (1)$$

where X = H_2 uptake in μmoles per gram of catalyst, W = the weight percentage of nickel, and f = the fraction of nickel reduced to the metal. Average crystallite diameters were calculated from $\% D$ assuming spherical metal crystallites, all having the same size d. Thus

$$d = 971/(\% D). \qquad (2)$$

Measurement of percentage reduction. The percentage of nickel reduced to the metallic state was determined by O_2 chemisorption at 723 K according to procedures described previously (*9*).

X-Ray diffraction measurements. X-Ray diffraction scans were obtained using a Phillips diffractometer with Cu$K\alpha$ radiation and a graphite monochrometer. The d values (interplanar spacings) for the various diffractogram peaks were calculated using the Bragg equation with λ = 0.15405 nm (Cu$K\alpha$ radiation) and n = 1. Metal particle sizes were estimated from X-ray line broadening using the Scherrer equation according to the methods of Klug and Alexander (*14*).

Electron microscopy measurements. Finely crushed samples were studied using a Hitachi HU-11E microscope. The powder was placed in *n*-butyl alcohol, more finely ground in a 7-ml tissue grinder, and then ultrasonicated to suspend the fine particles. A drop of the suspension was transferred to a Formvar-coated, copper grid. The alcohol was than evaporated leaving fine particles ready for observation. Micrographs were photographically enlarged to a magnification of 370,000×.

RESULTS

Chemisorption uptakes of H_2 at 298 K and of CO at either 190 or 273 K for alumina, alumina- and silica-supported

TABLE 1

Hydrogen and Carbon Monoxide Chemisorption Data for Alumina- and Silica-Supported Nickel

Catalyst	H_2 uptake[a] (μmoles/g)	CO uptake[b] (μmoles/g)	CO/H[c]
Al_2O_3 (Kaiser)	0.5	26[d]	52
Ni/Al_2O_3			
0.5%	0.8	44	28
1.0	4.6	189	9.9
2.9[e]	37	268	3.6
3	36	134[d]	1.9
9	108	247[d]	1.1
14	188	357[d]	0.95
23	283	453[d]	0.8
100% Ni (INCO)	4.5	4.9[d]	0.55
Ni/SiO_2			
2.7%	85	550	3.2
3.6[e]	81	183	1.1
13.5[e]	442	976	1.1
15	217	1290	3.0

[a] Total H_2 adsorption uptake at 298 K. Experimental accuracy estimated at ±10–15%.

[b] Irreversible CO adsorption uptake at 273 K (unless otherwise noted) corrected for physical and chemical adsorption on the support.

[c] Molecules CO adsorbed per atom of hydrogen adsorbed.

[d] CO adsorption at 190 K. Data represent the average of 2–3 runs; experimental accuracy was ±10–15%.

[e] Prepared by precipitation.

nickel, and unsupported nickel (INCO) are listed in Table 1 along with ratios of the number of CO molecules adsorbed per hydrogen atom adsorbed. Typical H_2 and CO isotherms are shown in Figs. 1 and 2, while CO/H ratios are plotted as functions of nickel loading and percentage reduction of nickel to the metal in Fig. 3.

From the data in Table 1, two trends are obvious for alumina-supported nickel catalysts: (i) H_2 and CO adsorption uptakes

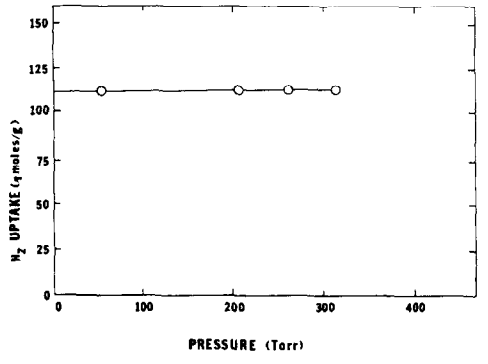

FIG. 1. H_2 uptake on 9% Ni/Al_2O_3 at 298 K.

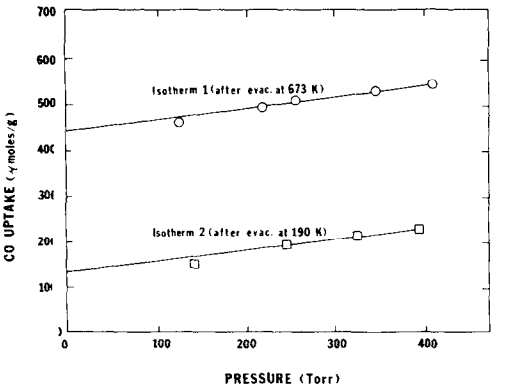

FIG 2. CO adsorption on 9% Ni/Al_2O_3 at 190 K. (○) Initial isotherm after evacuation at 673 K; (□) second isotherm after evacuation at 190 K.

increase with increased loading as might be expected and (ii) CO/H ratios decrease with increased metal loading, values ranging from 28 for 0.5% Ni/Al_2O_3 to 0.8 and 0.55 for 23% Ni/Al_2O_3 and 100% Ni, respectively, although the decrease is not linear as shown by Fig. 3. No such trend is apparent for Ni/SiO_2 catalysts; rather CO/H values are approximately unity for catalysts prepared by precipitation and 3 times larger for catalysts prepared by impregnation.

Table 2 lists values of percentage reduction of nickel to the metallic state determined by O_2 chemisorption and of crystallite diameter calculated from H_2 adsorption uptakes in Table 1. The estimates of nickel crystallite size from H_2 adsorption are also compared in Table 2 with values determined by X-ray diffraction and transmission electron microscopy. In most cases the agreement among the three techniques is excellent (within 10%) and in all cases good (within 30%). Three trends are apparent from the data in Table 2 for Ni/Al_2O_3 catalysts: (i) increasing percentage reduction of nickel to the metal, (ii) decreasing dispersion, and (iii) increasing metal crystallite diameter, all with increasing nickel loading. Figure 3 shows that increasing percentage reduction also correlates, albeit nonlinearly, with decreasing values of CO/H.

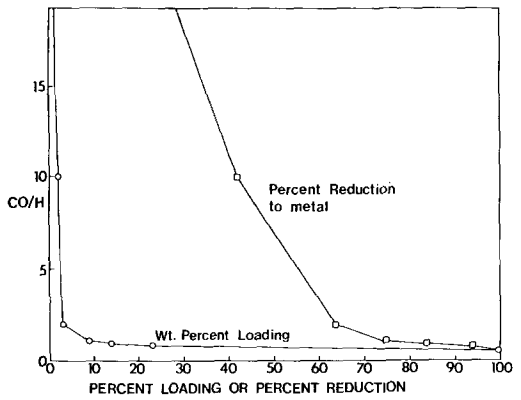

FIG. 3. CO/H ratio as a function of nickel loading and percentage reduction to the metal for impregnated Ni/Al_2O_3.

Values of H_2 uptake at 298 K and CO adsorption at 195, 273, and 294 K for 3% Ni/Al_2O_3 listed in Table 3 reveal that CO uptakes and CO/H values (referenced to H_2 adsorption at 294 K) decrease significantly with increasing temperature. After each CO adsorption measurement, the catalyst sample (still at the adsorption temperature) was evacuated 10–15 min through a special sidearm trap at 77 K; the evacuation was continued another 15–20 min while heating the sample to approximately 325 K. The collected volatiles were then driven off by purging with H_2 while heating the sidearm trap to about 325 K; this stream was directed through an electrically heated tube at 573 K in order to decompose any $Ni(CO)_4$ present in the gas to nickel metal. The tube was subsequently analyzed by atomic absorption for nickel. The results of

TABLE 2

Values of Dispersion, Percentage Reduction, and Average Crystallite Diameter for Alumina- and Silica-Supported Ni

Catalyst	Percentage reduction[a]	% D[b]	Average crystallite diameter (nm)		
			H_2 adsorption[c]	X-Ray[d]	Electron microscopy[e]
Ni/Al_2O_3					
0.5%	29	6.4(59)[g]	15(1.6)[g]	—	—
1.0	42	13(42)[g]	7.6(2.3)[g]	—	—
2.9[f]	68	22	4.5	—	—
3	64	22	4.4	—	—
9	75	19	5.2	—	—
14	84	17	5.6	5.7(200)	3.7, 4.6
23	94	15	6.3	5.3(200)	
Ni/SiO_2					
2.7%	71	51	1.9	—	2.9
3.6[f]	71	37	2.6	—	2.7
13.5[f]	93	41	2.4	<3[h](111)	2.9
15	90	19	5.1	9.7(111)	9.7, 12.1

[a] Based upon O_2 uptake at 725 K assuming formation of NiO.

[b] Based upon total H_2 uptake at 298 K and corrected for the amount reduced to metal. D = dispersion or fraction of metal exposed.

[c] Based upon total uptake at 298 K; corrected for the amount of nickel reduced to the metal.

[d] From X-ray diffraction line broadening. Miller indices of the pertinent diffraction peak are shown in parentheses.

[e] Averages determined from surface-area-weighted and volume-weighted crystallite size distributions.

[f] Prepared by precipitation. All other catalysts were prepared by impregnation.

[g] Percentage dispersion and average crystallite diameter shown in parentheses are based on CO adsorption, assuming that $CO/Ni_s = 3$ and that no CO adsorbs on unreduced nickel.

[h] X-ray amorphous; line broadening technique can be used to determine average particle diameter greater than 3 nm.

TABLE 3

CO Adsorption on 3% Ni/Al_2O_3 and Formation of $Ni(CO)_4$ as a Function of Temperature

Temp. (K)	H_2 uptake[a] (μmoles/g)	CO uptake[b] (μmoles/g)	CO/H[c]	Ni from $Ni(CO)_4$[d] Decomposition (g/g Ni)
298	30.8			
195		146	2.4	ND[e]
273		110	1.8	ND
294		88	1.4	0.077

[a] Total adsorption uptake.
[b] Irreversible uptake corrected for physical and chemical adsorption on the support.
[c] Molecules CO adsorbed per atom hydrogen adsorbed at 294 K.
[d] Collected by decomposition in an electrically heated tube and analyzed by atomic absorption.
[e] Not detectable.

this analysis listed in the last column of Table 3 indicate that detectable amounts of $Ni(CO)_4$ were produced only at the highest temperature of adsorption, 294 K.

DISCUSSION

H_2 Adsorption on Supported Nickel

Although previous workers (*15–17*) assumed an adsorption stoichiometry of one hydrogen atom per nickel surface atom ($H/Ni_s = 1$), this assumption was based on very limited and/or questionable data. For example Yates *et al.* (*15*) assumed $H/Ni_s = 1$ for supported nickel catalysts at 298 K on the basis of work by O'Neill (*18*) on an unsupported nickel powder of very low surface area. Brooks and Christopher (*16*) reported that $H/Ni_s = 1$ from comparison of nickel areas based on hydrogen chemisorption data at 523 K and X-ray line broadening for several poorly dispersed commercial Ni catalysts ($\%D = 1–7\%$). Unfortunately their estimates from the two different techniques varied by as much as 200–300%; moreover, their estimates of metal area from X-ray line broadening for a given sample varied by as much as 200–300%. Their H_2 adsorption data obtained at 525 K are of questionable validity since Schuit and van Reijen (*19*) have shown that H_2 adsorption decreases significantly with increasing temperature, and at 525 K the adsorption is essentially reversible. In fact, the H_2 uptakes for some of the samples of Brooks and Christopher were a factor of 10 less at 525 K compared to 298 K. Magnetic data discussed by Selwood (*17*) provide more convincing evidence of $H/Ni_s = 1$ but were nevertheless limited to only one Ni/Al_2O_3 catalyst and a series of Ni–Cu alloys having very similar dispersions.

The results of this study provide for the first time comprehensive, quantitative data to support the assumption of $H/Ni_s = 1$ for a wide range of nickel dispersions and loadings. That is, the good to excellent agreement among values of average crystallite diameter estimated from H_2 chemisorption, X-ray line broadening, and transmission electron microscopy (TEM) in Table 2 indicates that the hydrogen atom to surface nickel atom ratio is indeed unity for room-temperature hydrogen adsorption on alumina- and silica-supported nickel. Based on the data from Table 2, this stoichiometry is apparently valid for nickel loadings of 3–23% and nickel dispersions of 15–50%. Recent adsorption and TEM studies of precalcined and sintered Ni/SiO_2 catalysts in our laboratory (*20, 21*) show this to be true at even lower dispersions. These results are also consistent with previously reported data from our laboratory (*7*) showing $H/Ni_s = 1$ for an unsupported nickel, having a dispersion of 0.05%. Thus, room-temperature hydrogen chemisorption is recommended as a quantitative technique for measuring nickel surface area for alumina- and silica-supported nickel catalysts.

However, due caution is recommended in extrapolating these results to nickel loadings lower than 3% or to nickel catalysts containing supports other than alumina or silica—for example Ni/TiO_2 or Ni/ZrO_2 where strong metal–support interactions may induce changes in adsorption stoichiometry (*22–25*). Indeed, the data in Tables 1 and 2 for 0.5 and 1.0% Ni/Al_2O_3

suggest that the adsorption stoichiometry of $H/Ni_s = 1$ is not valid at nickel loadings lower than 3%, since (i) the H_2 uptakes and dispersions based on H_2 uptakes for these samples are unexpectedly low (one hardly expects metal dispersion to decrease with decreasing metal loading) and (ii) the CO/H ratios of 28 and 9.9 for these catalysts are unexpectedly high. It is not reasonable to conclude from these data that $CO/Ni_s = 28$ and 9.9, since nickel can coordinate with no more than three other CO molecules, if it is bonded to other Ni atoms (or to four other CO molecules if it is in the gas phase). Accordingly the most reasonable explanation for these phenomena is that strong metal–support interactions reduce the amount of H_2 adsorbed on Ni/Al_2O_3 at very low loadings in a manner similar to that observed for Ni/TiO_2 (*21, 25*).

Finally, one should not assume that the stoichiometry reported here for *total* hydrogen adsorption on nickel and determined in a *static,* volumetric system applies also to data obtained using *flow* techniques, by means of which *irreversible* rather than total adsorption is measured. In fact, we determined in this study that approximately 40% of the hydrogen was adsorbed reversibly at room temperature on 14% Ni/Al_2O_3 (i.e., could be removed by evacuation at 298 K). Slinken *et al.* (*26*) have shown that the amount of irreversibly adsorbed H_2 on Ni/SiO_2 catalysts varies significantly with temperature and nickel crystallite size.

A comment regarding our calculation of nickel dispersion and average crystallite diameter is appropriate here. In the case of most supported noble metals such as Pt/Al_2O_3 etc., it is customary to assume that all of the metal in the reduced catalyst is present as tiny metal crystallites. However, in base metal catalysts such as Ni/Al_2O_3 and Fe/Al_2O_3 a substantial fraction of the nickel or iron may be present as an oxide, which because of its strong interaction with the support is impossible to reduce completely to the metal at typical reduction temperatures (e.g., 673–773 K). A number of Mössbauer studies (*27–29*) provide evidence that the unreduced iron is intimately associated with the support as a phase separate from reduced metal crystallites. Recent ESCA work (*30*) shows the same to be true of commercial Ni/SiO_2 and Ni/Al_2O_3 catalysts. Thus, we believe our assumption that the unreduced nickel is present as a separate phase and that metal dispersion and crystallite size estimates should include a correction for this unreduced phase is based on sound experimental evidence.

Since in the case of the 0.5 and 1.0% Ni/Al_2O_3 catalysts metal dispersions calculated from hydrogen adsorption were unreasonably low, values were estimated from CO adsorption data assuming a stoichiometry of $CO/Ni_s = 3$ (the upper limit of CO adsorption on a nickel surface) and no adsorption on unreduced nickel sites. These assumptions are discussed in detail below. The estimates of nickel dispersion obtained by this approach of 59 and 42% for the 0.5 and 1.0% samples, respectively, are considered to be lower bounds since the CO/Ni_s ratio could be less than 3.

CO Adsorption on Supported Ni

Although adsorption of CO on supported nickel has received considerable attention (*16, 19, 31–36*), the effects of adsorption pressure, temperature, metal loading, degree of reduction, and metal dispersion on adsorption stoichiometry have not heretofore been quantitatively considered, with the exception of one of these studies (*35*). In their ir/magnetic study of well-characterized Ni/SiO_2 catalysts Primet *et al.* (*35*) investigated some of these effects, although their experiments did not cover the ranges of dispersion and metal loading surveyed by this study.

Effects of pressure and temperature. Early in this study it was determined that CO uptake depended significantly on equilibration pressure below 100–200 Torr, but that equilibrium adsorption could be obtained within 30–45 min at pressures ex-

ceeding 300–400 Torr (*4, 13, 37, 38*). Thus much of the previously reported adsorption data determined at 1–100 Torr are possibly suspect because they were not obtained at equilibrium.

The data in Table 3 show that the quantity of CO adsorbed irreversibly on nickel decreases with increasing temperature from 195 to 294 K. Assuming that $H/Ni_s = 1$, the values of CO/H represent also the number of CO molecules adsorbed per nickel surface atom. Thus, approximately $2\frac{1}{2}$ molecules of CO adsorb on each nickel surface atom in the 3% Ni/Al_2O_3 catalyst at 195 K; on the average of 1.8 and 1.4 CO molecules adsorb irreversibly on this catalyst at 273 and 294 K, respectively. It should also be mentioned that the magnitude of the second CO isotherm used to correct for physical adsorption on the support decreased very significantly with increasing temperature for a given catalyst as might be expected. Indeed, at 190 K, the amount of physically adsorbed CO was large (for example see Fig. 2); thus, unfortunately, the calculation of chemisorbed CO involved taking the difference between two large numbers. At 273 and 298 K significantly smaller amounts of physically adsorbed CO were observed. However, the data in Table 3 show that $Ni(CO)_4$ formation is significant at 298 K but not at 273 K in agreement with previous work (*19, 39, 40*). We therefore recommend 273 K as the optimum temperature for measuring CO adsorption on nickel.

One additional comment should be made in regard to technique. It was apparent from our survey of the literature that some authors considered and corrected for chemisorption on the support while others did not. On SiO_2 we determined H_2 and CO chemisorption to be negligible. As shown by the data in Table 1, H_2 adsorption on Al_2O_3 is very small; however, CO adsorption on Al_2O_3 is quite significant. The data for H_2 and CO adsorption on Al_2O_3 in Table 1 are in very good agreement with previous work (*39, 41*).

Effects of metal crystallite size and support. Although a few of the previous workers considered the effects of metal crystallite size (*31, 33–35*) and metal–support interactions (*32*) on CO adsorption their results were obviously in significant disagreement as to the qualitative nature of these effects; moreover, none of the previous work provided a quantitative measure of these effects on CO adsorption stoichiometry. For example, Yates and Garland (*31*) concluded from their ir and X-ray studies that CO is adsorbed as a single linear species with ir bands above 2000 cm^{-1} on well-dispersed Ni/Al_2O_3 and as a bridged species with ir bands below 2000 cm^{-1} on poorly dispersed Ni/Al_2O_3. However, van Hardeveld and Hartog (*33*) suggested that for their Ni/SiO_2 catalysts, bands above 2000 cm^{-1} be assigned to high coordination characteristic of large crystallites and bands below 2000 cm^{-1} be assigned to low coordination characteristic of edges, corners, etc., predominant in small crystallites, a conclusion exactly opposite to that of Yates and Garland. Primet *et al.* (*35*), on the other hand, concluded from their ir/magnetic data for Ni/SiO_2 catalysts that the fraction of linear and bridged sites is independent of metal crystallite size. Thus Yates and Garland (*31*) predict decreasing, van Hardeveld and Hartog (*33*) increasing, and Primet *et al.* (*35*) unchanging CO/Ni_s ratios with increasing nickel crystallite size.

The results of this study provide quantitative evidence that CO/Ni_s values decrease with increasing nickel crystallite size for Ni/Al_2O_3. That is, assuming $H/Ni_s = 1$, the CO/Ni_s values for Ni/Al_2O_3 range from 1.9 for $d = 4.4$ nm (3% Ni/Al_2O_3) to 0.8 for $d = 6.3$ nm (23% Ni/Al_2O_3) to 0.55 for $d =$ 2000 nm (100% Ni), as shown by data in Tables 1 and 2. Thus our results agree qualitatively with those of Yates and Garland (*31*), although on the basis of linear and bridged adsorption alone, their results would not predict CO/Ni_s values above 1.0.

Even though a good correlation is evident, one is not warranted in assuming that the changes in CO/Ni_s stoichiometry are a

result only of changes in metal crystallite size, since CO/H and CO/Ni_s ratios can also be correlated with metal loading and extent of reduction to the metallic state. In other words, the changes in CO adsorption stoichiometry may also be affected by metal–support interactions. This will be discussed in some detail below.

First, however, we wish to interpret the basis for the changes in CO/Ni_s ratio as a function of particle size in the light of recent ir studies (*35, 36*). These along with other previous ir studies establish the presence of four different kinds of adsorbed CO species on supported nickel: bridged or multicenter, linear, subcarbonyl, and CO adsorbed on Ni^{2+} or NiO. The characteristic structures and ir bands are summarized for these species in Table 4. Since the binding energy increases with decreasing wavenumber, the bridged species should be most strongly adsorbed and that on NiO least strongly held; indeed, this has also been confirmed by the earlier studies (*35–36*).

We hypothesize that:

(i) CO adsorbs principally as a subcarbonyl species, $Ni(CO)_x$, where $x = 2, 3$, on very small, two-dimensional nickel crystallites. This hypothesis is supported by the large CO/Ni ratios observed for the well-dispersed, low-loading catalysts in this study and the observation of a band at 2070–2090 cm^{-1} for well-dispersed nickel by several workers (*31, 33–36*). This band is apparently not present for poorly dispersed nickel (*31, 33*). Moreover, $Ni(CO)_4$ is more easily formed in the case of these small particles (*33*). It is also reasonable that multiple adsorption would be facilitated on small crystallites having a large fraction of high-coordination sites. In fact, recent studies (*42, 43*) have shown evidence for adsorption of subcarbonyl species on alumina-supported Rh catalysts having low metal loadings of small crystallites present in raftlike structures on the support.

(ii) CO adsorbs on large, highly crystalline, three-dimensional nickel crystallites in

TABLE 4

Surface CO Species Chemisorbed on Supported Ni and Their Assigned Infrared Bands[a]

Infrared frequency (cm^{-1})	Species	Site	Strength of adsorption
1960	Bridged: 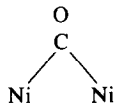	Poorly dispersed, crystalline	Very strong
2030–2050	Linear: 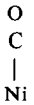	Moderately dispersed Ni	Strong
2065–2090	Subcarbonyl: 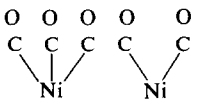	Well-dispersed Ni	Weak to fairly strong
2195	Ni^{2+}: 	Partially reduced catalysts	Weak

[a] Adapted from Refs. (*35, 36*).

the bridged or multicentered form. This hypothesis is well supported by our data for high-loading and unsupported nickel catalysts and by ir studies of supported nickel (*31, 35, 36*) and unsupported, single-crystal nickel (*44*).

(iii) In moderately dispersed nickel catalysts, a combination of bridged, linear, and subcarbonyl adsorption is observed. As the dispersion is increased less bridged and more linear/subcarbonyl species are observed. This hypothesis accounts then for the increasing CO/Ni_s ratio with decreasing particle size evident in Tables 1 and 2. These variations in CO/H ratio and strength of adsorption as a function of dispersion can have a significant impact on activity and selectivity (*45*).

Although the above listed hypotheses have been discussed in terms of changes in metal crystallite size, it is evidently also possible to relate the changes in CO adsorption stoichiometry to metal–support interactions, the importance of which varies with metal loading and the extent of which is related to the reducibility of the catalysts, i.e., extent of reduction to the metal. Thus at low metal loadings, a large fraction of the metal is in intimate contact with the support, accounting for the relatively low extent of reduction and the presence of small crystallites. Since these small metal particles are in intimate, direct contact with the support their geometrical shape and electronic properties may be markedly influenced by the strong metal–support interaction (*42, 43, 45*). This could result in a relatively weaker bond between CO and nickel, as observed in the ir studies of subcarbonyl species on small particles. In the case of high-loading catalysts, a smaller fraction of the nickel is in direct contact with the support and thus a larger fraction of the nickel is more easily reduced to three-dimensional crystals with a smaller degree of interaction with the support. The above explanation accounts for the correlation of CO/H with percentage reduction to the metal in Fig. 3. Moreover, the ambiguity of separating the effects of particle size and metal–support interactions on adsorption properties is evident.

Thus far we have considered only the adsorption on nickel metal crystallites. What about CO adsorption on the Ni^{2+} or NiO sites? If one molecule of CO adsorbed on each Ni^{2+} site, CO/H ratios would increase dramatically with decreasing extent of reduction, since hydrogen chemisorbs to a relatively small extent on NiO or Ni^{2+} compared to the metal (*7*). Such an effect could by itself explain the increasing CO/Ni_s values with decreasing percentage reduction shown in Fig. 3. However, two separate pieces of experimental evidence suggest that the quantity of CO adsorbing on the unreduced sites in these catalysts was probably negligible relative to CO adsorption on the metal: (i) in this study CO adsorption on a sample of 3% Ni/Al_2O_3 calcined in air at 573 K for 2 h was determined to be the same within experimental error as on the support, and (ii) Primet *et al.* (*35*) observed that the peak at 2195 cm^{-1} corresponding to adsorption of CO on Ni^{2+} was observed only in samples with less than 5% of the nickel reduced to the metal; moreover, the area of the peak at 2185 cm^{-1} for the sample having a degree of reduction of 5% was approximately 2 orders of magnitude smaller than the peak areas for CO adsorption of nickel metal.

Brooks and Christopher (*16*) cited their large CO/H ratios for alumina-and zeolite-supported nickel as evidence that CO adsorbs selectively on Ni^{2+} or NiO. They recommend the use of a combination of CO and H_2 adsorption with X-ray diffraction to determine surface Ni and Ni^{2+}. The results of this study provide an alternative explanation for their large CO/H ratios, namely, subcarbonyl formation in their CO adsorption measurements coupled with substantially less than monolayer H_2 adsorption on reduced nickel at 525 K. Moreover, the application of their technique to the data in this study leads to altogether unreasonable values of percentage reduction and percent-

age dispersion, e.g., values of percentage reduction of 4, 10, and 28 for 0.5, 1, and 2.9% Ni/Al_2O_3 and values of 31 and 34% for 2.7 and 15% Ni/SiO_2, respectively. These values are unrealistically low for either Ni/Al_2O_3 or Ni/SiO_2 catalysts and at significant variance with our O_2 adsorption data. Consistent with their approach nickel metal dispersions for 2.7 and 15% Ni/SiO_2 are calculated from Eq. (1) to be 120 and 50%, respectively. The former value is, of course, impossible, while the second value leads via Eq. (2) to an estimated average nickel crystallite diameter of 2.0 nm for 15% Ni/SiO_2, a factor of 5 lower than observed by X-ray diffraction and electron microscopy (see Table 2). In view of these problems, because the amount of CO adsorption on Ni^{2+} is apparently relatively small compared to adsorption on the metal and since the effects of different system variables such as temperature and pressure and of catalyst properties such as dispersion, support, etc., on adsorption stoichiometry of CO on Ni^{2+} are unknown, the proposed technique of Brooks and Christopher is questionable.

Effects of preparation. From the data in Tables 1 and 2 it is obvious that significant differences in adsorption properties are observed for catalysts of the same loading prepared by different techniques. Most notably the values of CO/H (hence values of CO/Ni_s) are significantly larger for Ni/SiO_2 catalysts prepared by impregnation relative to those prepared by precipitation. The particle size distributions of the impregnated catalysts are significantly broader than those prepared by controlled pH precipitation (*21*, *46*). In other words there is probably a larger proportion of very small and very large particles in the impregnated catalysts, the very small ones contributing most significantly to larger values of CO adsorption and hence large CO/H ratios. However, in the case of alumina-supported nickel, the CO/H value for the precipitated 2.9% Ni/Al_2O_3 is twice as large as that for the impregnated 3.0% Ni/Al_2O_3, suggesting a larger proportion of small particles in the precipitated catalyst. The significant differences in CO/H ratio for the 3% catalysts on the alumina and silica supports prepared by impregnation and precipitation, respectively, illustrate the importance of metal–support interactions in determining adsorption behavior. The precipitated Ni/Al_2O_3 and Ni/SiO_2 catalysts evidence the behavior anticipated, assuming the nickel–alumina interaction to be stronger than that for nickel–silica (*32*) and hence the Ni–CO bond to be stronger in the latter case.

CONCLUSIONS

(i) Hydrogen adsorbs dissociatively on alumina-and silica-supported nickel at 298 K with a stoichiometry of one hydrogen atom per nickel surface atom. This stoichiometry is apparently valid over wide ranges of dispersion and nickel loadings above 3 wt%. Hydrogen adsorption at 298 K is recommended as a convenient, general technique for measuring nickel metal surface area in supported nickel catalysts.

(ii) CO adsorption on nickel is considerably more complex, the stoichiometry varying with temperature, metal dispersion, metal loading, and preparation. Although CO adsorption is not recommended as a technique to measure nickel surface area, it can be used as a probe to study particle size effects and metal–support interactions, since the adsorption stoichiometry is a sensitive measure of these effects. CO adsorption at 273 K minimizes corrections necessary for physical adsorption, while avoiding $Ni(CO)_4$ formation.

ACKNOWLEDGMENTS

The authors gratefully acknowledge technical assistance by Dr. Charles Pitt of the Department of Metallurgy, University of Utah, for X-ray analysis. We also express thanks to Joseph Oliphant, Ken Atwood, Richard Fowler, Scott Engstrom, John Watkins, Paul Moote, and Jay Butler for technical assistance and to Donald Mustard for electron microscopy measurements. We are also grateful to Kyung Sup Chung and Donald Stowell who performed some of the early CO

adsorption experiments leading to this study. Support of this work by the Energy Research and Development Administration (Contract EX-76-S-01-1790), the Department of Energy (Contract EF-77-S-01-2729), and the National Science Foundation (ENG 75-00254) is likewise gratefully acknowledged.

REFERENCES

1. Mills, G. A., and Steffgen, F. W., *Catal. Rev.* **8,** 159 (1973).
2. Vannice, M. A., *Catal. Rev.* **14**(2), 153 (1976).
3. "Methanation of Synthesis Gas," Advan. Chem. Ser. Vol. 146, 1975.
4. Bartholomew, C. H., "Alloy Catalysts with Monolith Supports for Methanation of Coal-Derived Gases," Final Report to ERDA, FE-1790-9, Sept. 6, 1977.
5. Bartholomew, C. H., "Alloy Catalysts with Monolith Supports for Methanation of Coal-Derived Gases," Annual Report to DOE, FE-2729-4, Oct. 5, 1978.
6. Farrauto, R. J., *AIChE Symp. Ser.* **70,** No. 143, 9–22 (1975).
7. Pannell, R. B., Chung, K. S., and Bartholomew, C. H., *J. Catal.* **46,** 340 (1977).
8. van Dillen, J. A., Geus, J. W., Hermans, L. A. M., and vander Meivben, J., *in* "Proceedings, 6th International Congress on Catalysis, London, 1976" (G. C. Bonds, P. B. Wells, and F. C. Tompkins, Eds.). The Chemical Society, London, 1977.
9. Bartholomew, C. H., and Farrauto, R. J., *J. Catal.* **45,** 41 (1976).
10. Bartholomew, C. H., "Alloy Catalysts with Monolith Supports for Methanation of Coal-Derived Gases," Quarterly Report to DOE, FE-2729-5, Jan. 5, 1979.
11. Bartholomew, C. H., "Alloy Catalysts with Monolith Supports for Methanation of Coal-Derived Gases," Quarterly Report to DOE, FE-2729-6, April 5, 1979.
12. Bartholomew, C. H., Ph.D. dissertation, Stanford University, 1972.
13. Bartholomew, C. H., "Alloy Catalysts with Monolith Supports for Methanation of Coal-Derived Gases," Quarterly Progress Report to ERDA, FE-1790-1, Aug. 6, 1975.
14. Klug, H. P., and Alexander, L. E., "X-ray Diffraction Procedures for Polycrystalline and Amorphous Materials." Wiley, New York, 1954.
15. Yates, D. J. C., Taylor, W. F., and Sinfelt, J. H., *J. Amer. Chem. Soc.* **86,** 2996 (1964).
16. Brooks, C. S., and Christopher, G. L. M., *J. Catal.* **10,** 211 (1968).
17. Selwood, P. W., *J. Catal.* **42,** 148 (1976).
18. O'Neill, C. E., thesis, Columbia University, 1961.
19. Schuit, G. C. A., and van Reijen, L. L., *Advan. Catal.* **10,** 242 (1958).
20. Sorenson, W. L., and Bartholomew, C. H., paper in preparation.
21. Mustard, D. G., and Bartholomew, C. H., *J. Catal.*, in press.
22. Tauster, S. J., Fung, S. C., and Garten, R. L., *J. Amer. Chem. Soc.* **100,** 170 (1978).
23. Vannice, M. A., and Garten, R. L., *J. Catal.* **56,** 236 (1979).
24. Sorenson, W. L., Mustard, D. G., and Bartholomew, C. H., paper in preparation.
25. Bartholomew, C. H., Pannell, R. B., Butler, J. L., and Mustard, D. G., paper presented at the 179th National Meeting of the ACS in Houston, March 23–28, 1980.
26. Slinken, A. A., Kucherov, A. V., and Rubinshtein, A. M., *Kinet. Catal. (USSR)* **19**(2), 415 (1978).
27. Delgass, W. N., and Boudart, M., *Catal. Rev.* **2,** 129 (1968).
28. Dumesic, J. A., Topsoe, H., Khammouma, S., and Boudart, M., *J. Catal.* **37,** 486 (1975).
29. Dumesic, J. A., and Topsoe, H., *Advan. Catal.* **26,** 121 (1977).
30. Shalvoy, R. B., Reucroft, P. J., and Davis, B. H., *J. Catal.* **56,** 336 (1979).
31. Yates, J. T., and Garland, C. W., *J. Phys. Chem.* **65,** 617 (1961).
32. O'Neill, C. E., and Yates, D. J. C., *J. Phys. Chem.* **65,** 901 (1961).
33. van Hardeveld, R., and Hartog, F., *Advan. Catal.* **75,** 86 (1972).
34. Derbeneva, S. S., Karakchiev, L. G., Kuznetsov, B. N., and Yermakov, Yu. I., *Kinet. Catal.* (USSR) **16,** 227 (1975).
35. Primet, M., Dalmon, J. A., and Martin, G. A., *J. Catal.* **46,** 25 (1977).
36. Rochester, C. H., and Terrell, R. J., *J. Chem. Soc. Trans. Faraday I* **73,** 609 (1977).
37. Chung, K. S., thesis, Brigham Young University, 1975.
38. Stowell, D. G., thesis, Brigham Young University, 1976.
39. Hughes, T. R., Houston, R. J., and Sieg, R. P., *Ind. Eng. Chem. Process Des. Develop.* **1,** 96 (1962).
40. Germain, J. E., Ostyn, M., and Benunfils, J. P., *J. Chem. Phys.* **61,** 686 (1964).
41. Wanke, S. E., and Dougharty, N. A., *J. Catal.* **24,** 367 (1972).
42. Yates, D. J. C., Murrell, L. L., and Prestridge, E. B., *J. Catal.* **57,** 41 (1979).
43. Yao, H. C., Japar, S., and Shelef, M., *J. Catal.* **50,** 407 (1977).
44. Burton, J. J., and Pugel, T. M., *J. Catal.* **47,** 280 (1977).
45. Bartholomew, C. H., Pannell, R. B., and Butler, J. B., *J. Catal.*, **65,** 335 (1980).
46. Richardson, J. T., and Dubus, R. J., *J. Catal.* **54,** 207 (1978).